ELECTRONICS AND ELECTRICAL ENGINEERING
ISSN 1392 – 1215 *2009. No. 8(96)*
ELEKTRONIKA IR ELEKTROTECHNIKA

ELECTRICAL ENGINEERING
T 190
ELEKTROS INŽINERIJA

Numerical Analysis of Spatial Force Components in Direct Current Corona Field

P. Marčiulionis, S. Žebrauskas
Department of Electrical Engineering, Kaunas University of Technology,
Studentų st. 48, LT-51367 Kaunas, Lithuania, phone:+370 37 300268; e-mail: stasys.zebrauskas@ktu.lt

Introduction

Corona discharge in air is frequently employed in charge transfer processes such as electrostatic painting , powder coating, separation of granular mixtures, dust precipitation, gas cleaning, enhancing of heat and mass exchange processes, spraying of liquids, etc. Fundamentals of corona discharge theory are known since the research works of Peek, Warburg, Townsend, Thomson, Deutsch, Kaptzov [1]. The phenomenon is widely used in industrial applications because of comparatively small energy consumption of corona field devices and ability to produce the desirable effect only by using the corona discharge. The system of corona field equations frequently is reduced to Poisson equation and the equation for charge density [2]. Generally there is no analytical solution for this problem. Exact solution exists only for the field of coaxial electrode system described as one-dimensional problem. Finite-difference and finite element methods are often used to solve Poisson equation and the method of characteristics and donor-cell method are used to solve the charge equation [1-3]. Ion-driven wind is the supplementary phenomenon of corona discharge and is often employed in industrial applications also. It is often used in numerous applications of electrohydraulics. Incompressible and viscous airflow induced by spatial (Coulomb) force is determined by Navier-Stokes equation and the equation of flow continuity. Spatial force there is assumed as the product of charge density and field strength. Finite-difference method is chosen for solving these equations in [4]. Polar system of coordinates and corresponding grid is used for wire-to-plane electrode system. It enables to reduce the number of grid nodes essentially. Finite-difference approximation of Navier-Stokes and continuity equations also is given there. Components of spatial force computed according analytical formulas based upon Deutsch‘s-Popkov‘s assumption are given in [5]. More detailed analysis show the correctness of these results only for coaxial electrode system with one-dimensional corona field. Therefore an algorithm for numerical computation of spatial force components is proposed in [6]. We discuss the procedure of computation and the results in this paper.

Finite-difference aproximation of corona field equations

The system of differential equations for electric field of direct current corona comprising the Poisson's and the continuity equations is the following [2, 6]:

$$\begin{cases} \Delta V = -\rho/\varepsilon, \\ \nabla\rho \cdot \nabla V = \rho^2/\varepsilon; \end{cases} \quad (1)$$

where V is the field potential, ρ is the volume density of space charge and ε is the dielectric permittivity. An expression of Poisson's equation in polar coordinate system is the sum of second partial derivatives in respect of coordinates r and φ:

$$\frac{1}{r}\cdot\frac{\partial}{\partial r}\left(r\frac{\partial V}{\partial r}\right)+\frac{1}{r^2}\cdot\frac{\partial^2 V}{\partial \varphi^2}=-\frac{\rho}{\varepsilon}. \quad (2)$$

Finite-difference approximation of this equation for irregular polar grid contains of potential differences related to distances between central grid node O and neighbouring nodes P, R, Q and S [6]:

$$\frac{V_{\mathrm{P}}}{a_{\mathrm{P}}\left(a_{\mathrm{P}}+a_{\mathrm{R}}\right)}+\frac{V_{\mathrm{R}}}{a_{\mathrm{R}}\left(a_{\mathrm{P}}+a_{\mathrm{R}}\right)}+$$

$$+\frac{V_{\mathrm{Q}}\left(2r+a_{\mathrm{S}}\right)}{2ra_{\mathrm{Q}}\left(a_{\mathrm{Q}}+a_{\mathrm{S}}\right)}+\frac{V_{\mathrm{S}}\left(2r-a_{\mathrm{Q}}\right)}{2ra_{\mathrm{S}}\left(a_{\mathrm{Q}}+a_{\mathrm{S}}\right)}=$$

$$=V_{\mathrm{O}}\left(\frac{1}{a_{\mathrm{P}}a_{\mathrm{R}}}+\frac{2r+a_{\mathrm{S}}-a_{\mathrm{Q}}}{2ra_{\mathrm{S}}a_{\mathrm{Q}}}\right)-\frac{\rho_{\mathrm{O}}}{\varepsilon}. \quad (3)$$

Distances a from the central node O to the neighbouring nodes P, Q, R and S are shown in Fig. 1. Equation (3) gives an acceptable accuracy for laplacian fields ($\rho = 0$), but it‘s accuracy is not satisfactory for

fields with space charge. Therefore we use the following approximation:

$$\frac{2V_{\mathrm{P}}}{a_{\mathrm{P}}^2+a_{\mathrm{P}}a_R}+\frac{2V_{\mathrm{Q}}}{a_{\mathrm{Q}}^2+a_Q a_{\mathrm{S}Q}}+\frac{2V_{\mathrm{R}}}{a_{\mathrm{R}}^2+a_{\mathrm{P}}a_R}+\frac{2V_{\mathrm{S}}}{a_{\mathrm{S}}^2+a_Q a_{\mathrm{S}Q}}-$$

$$-2V_0\left(\frac{1}{a_{\mathrm{Q}}a_{\mathrm{S}}}+\frac{1}{a_{\mathrm{P}}a_{\mathrm{R}}}\right)=\frac{\rho_{\mathrm{O}}}{\varepsilon}. \qquad (4)$$

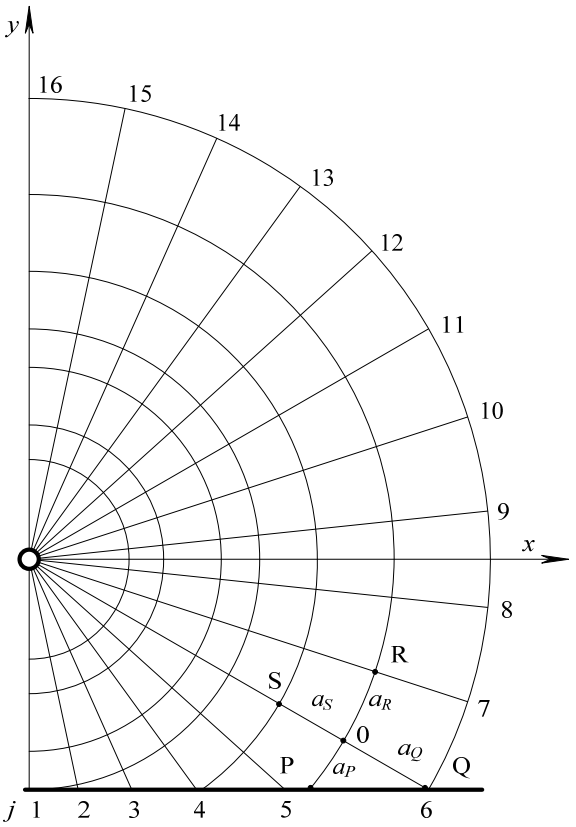

Fig. 1. Polar grid for the area of computation

Components of field strength:

$$\frac{\partial V}{\partial r}=-\frac{V_{\mathrm{S}}a_{\mathrm{Q}}}{a_{\mathrm{S}}\left(a_{\mathrm{Q}}+a_{\mathrm{S}}\right)}+\frac{V_{\mathrm{Q}}a_{\mathrm{S}}}{a_{\mathrm{Q}}\left(a_{\mathrm{Q}}+a_{\mathrm{S}}\right)}+\frac{V_{\mathrm{O}}\left(a_{\mathrm{Q}}-a_{\mathrm{S}}\right)}{a_{\mathrm{Q}}a_{\mathrm{S}}}, \qquad (5)$$

$$r\frac{\partial V}{\partial \varphi}=-\frac{V_{\mathrm{P}}a_{\mathrm{R}}}{a_{\mathrm{P}}\left(a_{\mathrm{P}}+a_{\mathrm{R}}\right)}+\frac{V_{\mathrm{R}}a_{\mathrm{P}}}{a_{\mathrm{R}}\left(a_{\mathrm{P}}+a_{\mathrm{R}}\right)}+\frac{V_{\mathrm{O}}\left(a_{\mathrm{P}}-a_{\mathrm{R}}\right)}{a_{\mathrm{P}}a_{\mathrm{R}}} \qquad (6)$$

Gradient of charge density:

$$\nabla\rho=\mathrm{grad}\rho=\sqrt{\left(\frac{\partial\rho}{\partial r}\right)^2+\left(r\frac{\partial\rho}{\partial\varphi}\right)^2}\ ; \qquad (7)$$

where

$$\frac{\partial\rho}{\partial r}=\frac{\rho_{\mathrm{Q}}a_{\mathrm{S}}}{a_{\mathrm{Q}}\left(a_{\mathrm{Q}}+a_{\mathrm{S}}\right)}-\frac{\rho_{\mathrm{S}}a_{\mathrm{Q}}}{a_{\mathrm{S}}\left(a_{\mathrm{Q}}+a_{\mathrm{S}}\right)}+\frac{\rho_{\mathrm{O}}\left(a_{\mathrm{Q}}-a_{\mathrm{S}}\right)}{a_{\mathrm{Q}}a_{\mathrm{S}}}, \qquad (8)$$

$$r\frac{\partial\rho}{\partial\varphi}=-\frac{\rho_{\mathrm{P}}a_{\mathrm{R}}}{a_{\mathrm{P}}\left(a_{\mathrm{P}}+a_{\mathrm{R}}\right)}+\frac{\rho_{\mathrm{R}}a_{\mathrm{P}}}{a_{\mathrm{R}}\left(a_{\mathrm{P}}+a_{\mathrm{R}}\right)}-\frac{\rho_{\mathrm{O}}\left(a_{\mathrm{P}}-a_{\mathrm{R}}\right)}{a_{\mathrm{P}}a_{\mathrm{R}}}. \qquad (9)$$

Final form of continuity equation:

$$\frac{\partial\rho}{\partial r}\cdot\frac{\partial V}{\partial r}+r\frac{\partial\rho}{\partial\varphi}\cdot r\frac{\partial V}{\partial\varphi}=\frac{\rho^2}{\varepsilon}. \qquad (10)$$

Boundary conditions

The main boundary conditions needed for the solution of corona field equations are the values of electrode potentials, the field strength E_0 on the surface of the wire corresponding to corona onset voltage U_0, and the space charge density ρ on the surface of the wire. Usually the potential of plane electrode is 0, the potential of wire electrode is U. There are many of ways to describe boundary condition for ρ on the surface r_0 [1-3]. We begin from $\rho(r, \varphi) = 0$ (Fig. 2) in all nodes of computing area of the field including the surface of the wire.

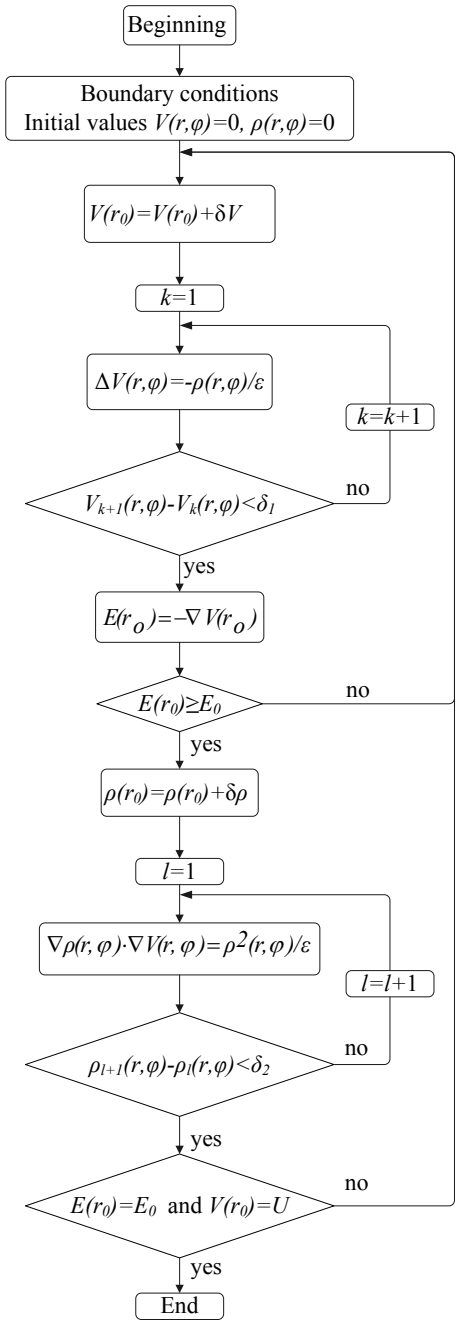

Fig. 2. Computational scheme for the numerical analysis of corona field

According the Kaptzov's asssumption the field strength on the wire surface $E(r_0)$ is equal to the initial field strength determined by Peek's formula [3] if the corona voltage U exceeds the discharge onset voltage U_0. Boundary condition for potential on the axies of symmetry j = 1 and j = 16 (Fig. 1) is $V_P = V_R$. The condition for potential on the free field border represented by the outer circle arc in Fig. 1 is the following:

$$V_Q = V_O^2 / V_S \,. \qquad (11)$$

Boundary condition for charge density on the surface on the corona wire is determined iteratively as it can be seen from Fig. 2. Charge density $\rho(r_0)$ is increased from the value $\rho = 0$ by the step $\delta\rho$ to the value corresponding the field strength condition $E(r_0) = E_0$. Boundary condition for wire potential is determined in the same way by increasing from $V(r_0) = 0$ with the step δV to the value $V(r_0) = U$. Procedure of computation of potentials and charge densities according (4) and (10) involves the iteration until convergence.

Test problem

The main difficulty for checking the computational results is to give the correct and adequate test problem. In the case of this paper we can construct the test problem only for Laplacian field. We use as the test problem an exact solution for the field of two infinite line charges $+\tau$ and $-\tau$ (Fig. 2). Electrostatic field of these two charges is the same as the field in wire-to-plane electrode system. The potential of an arbitrary point M may be expressed as a superposition of potentials $V_{+\tau}$ and $V_{-\tau}$:

$$V_M = V_{+\tau} + V_{-\tau} = \frac{\tau}{2\pi\varepsilon} \cdot \ln\frac{r''}{r'} + C, \qquad (12)$$

where ε is the permittivity of the space, r' and r'' are the distances from the point M to the charges $+\tau$ and $-\tau$ (Fig. 3). For the point N: $x_N = 0$, $y_N = -h$, $V_N = 0$, $r'_N = r''_N = b = \sqrt{h^2 - r_0^2}$, $\ln(r_{-\tau}/r_{+\tau}) = 0$, $C = 0$. For the point A: $x_A = 0$, $y_A = -r_0$, $V_A = U$, $r'_A = b - h + r_0$, $r''_A = b + h - r_0$, $(\tau/2\pi\varepsilon)\cdot\ln(r''_A/r'_A) = U$. Therefore

$$k_\tau = \frac{\tau}{2\pi\varepsilon} = \frac{U}{\ln(b + h - r_0)/(b - h + r_0)} \,. \qquad (13)$$

If the cartesian coordinates of the point M are x and y the distances between M and the line charges and may be written $r' = \sqrt{x^2 + (y + h - b)^2}$, $r'' = \sqrt{x^2 + (y + h + b)^2}$. Then, for polar coordinates, Laplacian field potential finally may be written as

$$V(r,\alpha) = k_\tau \cdot \ln\frac{\sqrt{(r\cos\alpha)^2 + (h + b + r\sin\alpha)^2}}{\sqrt{(r\cos\alpha)^2 + (h - b + r\sin\alpha)^2}}. \qquad (14)$$

The field strength vector for polar coordinates is

$$\boldsymbol{E}(r,\alpha) = -\left[\frac{\partial V(r,\alpha)}{\partial r}\cdot\boldsymbol{e}_r + \frac{1}{r}\cdot\frac{\partial V(r,\alpha)}{\partial\alpha}\cdot\boldsymbol{e}_\alpha\right]. \qquad (15)$$

After differentiating the potential the field strength components are the following:

$$E_r = k_\tau\left[\frac{r + n\sin\alpha}{r^2 + 2rn\sin\alpha + n^2} - \frac{r + m\sin\alpha}{r^2 + 2rm\sin\alpha + m^2}\right], \qquad (16)$$

$$E_r = k_\tau\left[\frac{n\cos\alpha}{r^2 + 2rn\sin\alpha + n^2} - \frac{m\cos\alpha}{r^2 + 2rm\sin\alpha + m^2}\right], \qquad (17)$$

where $m = h + b$, $n = h - b$.

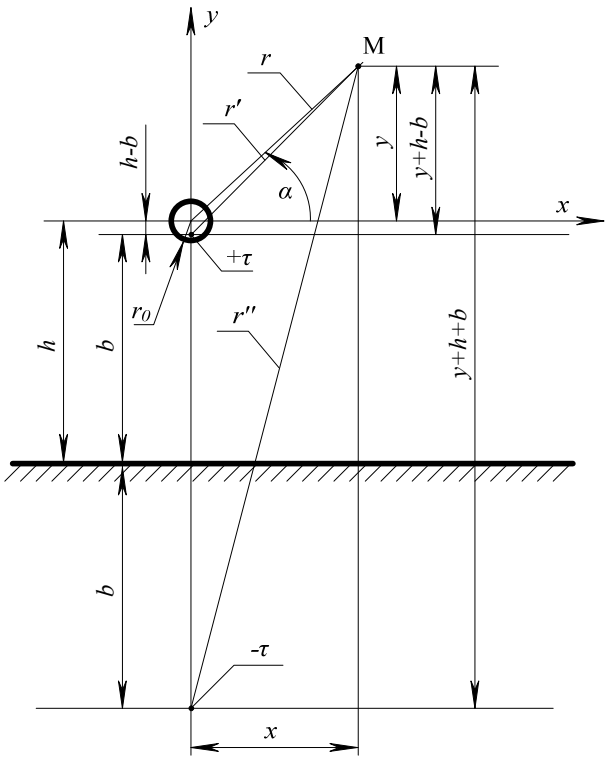

Fig. 3. Electrostatic field of two infinite line charges $+\tau$ and $-\tau$

Results of computation

Parameters of wire-to-plain electrode system are the following: radius of the wire r_0 = 0,05 mm, spacing between the wire and the plane electrode h = 12,0 mm, voltage U = 10,0 kV, ion mobility k = 2,20 cm^2/Vs. Characteristic parameter of polar grid m = 15, it corresponds to the central angle between neighbour lines φ_0 = 12° (0,209 rad). Number of nodes in computational area shown in Fig. 1 is 518. The law of changing of coordinate r is the same as in [6]. Program is written in Pascal language by using Delphi medium.

Results of electrostatic field (0 in the right side of Poissons equation) computation are shown in Table 1. Data of 3rd and 5th columns correspond to potential and field strength distribution on the symmetry axis of the field (line j= 1) computed according to digital procedure. The 2nd and the 4th columns of the table contain corresponding data determined by analytical formulas (14)

and (16). Coincidence of digital data with analytical ones is good. Maximum difference of potential at the surface of the wire is only 0,13 %, and it is 6,4 % for field strength. These differences may be reduced by increasing the number of nodes in the grid. It shows the reliability of presented procedure for computation of nonhomogeneous electrostatic fields.

Table 1. Electrostatic field potential and field strength on the symmetry axis

r, mm	V, V accrd. (14)	V, V, acc. (1), $\rho = 0$	E, kV/cm accrd.(16)	E, kV/m (1), $\rho = 0$
0,050	10000	10000	324,627	310,352
0,060	9688	9675	268,553	285,639
0,073	9379	9351	222,145	235,399
0,088	9070	9028	183,793	194,027
0,107	8761	8706	152,083	159,955
0,129	8451	8385	125,865	131,891
0,156	8141	8065	104,187	108,776
0,189	7831	7746	86,264	89,735
0,229	7520	7427	71,444	74,051
0,279	7209	7109	59,192	61,130
0,335	6897	6791	49,061	50,486
0,405	6584	6474	40,686	41,718
0,490	6270	6156	33,362	34,495
0,592	5955	5839	28,037	28,546
0,716	5639	5521	23,306	23,645
0,866	5320	5202	19,395	19,608
1,048	4999	4882	16,163	16,285
1,267	4676	4561	13,493	13,548
1,533	4349	4236	11,288	11,296
1,854	4018	3909	9,469	9,445
2,242	3681	3578	7,969	7,923
2,712	3338	3241	6,734	6,675
3,280	2986	2896	5,721	5,654
3,966	2623	2542	4,892	4,822
4,797	2247	2175	4,220	4,148
5,802	1852	1791	3,682	3,611
7,017	1432	1383	3,262	3,193
8,486	977	943	2,953	2,883
10,26	472	455	2,757	2,682
12,00	0	0	2,699	2,620

Data of corona field strength and charge density on the axis of the field are given in Table 2. Digital results are presented in 3rd and 5th columns, and data determined by analytical formulas based upon Deutsch‘s -Popkov‘s assumption (the space charge of corona field changes only a modulus of field strenght vector but not its direction) [6] correspond to 2nd and 4th columns. Comparison of these data is only qualitative because of dificulty to evaluate the correctness of data computed by analytical formulas. It is performed to determine the approximate quantities. Difference of corona field strength varies from 0,3 % at the surface of the wire to 10,7 % on the surface of the plate. Comparison of data given in Table 1 and Table 2 show that the space charge reduces the field strength at the surface of corona wire and increases it at the surface of plane electrode. This phenomenon is well known since the investigations of first researchers. Corresponding differences for charge density is 8,1 % and 16,7 %. It confirms the conclusion of researchers [1-3] about the crucial character of determination of ρ to the results of computation.

Table 2. Corona field strength and charge density on the symmetry axis

r, mm	E, kV/cm accord.[6]	E, kV/cm (1), (5)	ρ, μC/m^3 accord.[6]	ρ, μC/m^3 (1), (5)
0,050	158,416	158,000	3214,2	2951,3
0,060	131,075	131,448	3213,3	2950,7
0,073	108,476	108,345	3212,1	2949,6
0,088	89,799	89,317	3210,3	2948,1
0,107	74,367	73,651	3207,6	2945,8
0,129	61,612	60,756	3203,8	2942,5
0,156	51,098	50,147	3198,2	2937,6
0,189	42,415	41,426	3190,0	2930,5
0,229	35,259	34,265	3178,2	2920,2
0,279	29,369	28,393	3161,2	2905,2
0,335	24,531	23,588	3136,9	2883,5
0,405	20,569	19,671	3102,4	2852,5
0,490	17,339	16,491	3054,1	2808,7
0,592	14,720	13,926	2987,6	2747,5
0,716	12,613	11,877	2898,2	2664,2
0,866	10,937	10,260	2781,3	2553,7
1,048	9,624	9,045	2634,3	2412,9
1,267	8,613	8,513	2457,3	2241,3
1,533	7,853	7,348	2254,6	2043,4
1,854	7,301	6,849	2034,2	1827,9
2,242	6,918	6,514	1806,8	1606,7
2,712	6,673	6,310	1582,9	1391,8
3,280	6,541	6,213	1371,7	1192,3
3,966	6,508	6,205	1179,1	1013,9
4,797	6,565	6,279	1008,2	858,9
5,802	6,716	6,434	859,8	726,8
7,017	6,978	6,683	733,3	615,9
8,486	7,388	7,054	626,8	523,9
10,26	8,029	7,602	538,7	448,4
12,00	8,848	7,898	478,6	398,4

Results of digital computation of charge density and (areal) current density on the surface of corona wire are given in Table 3. Linear current density may be determined by integration the areal density:

$$I_0 = \int_S \boldsymbol{J} \cdot \mathrm{d}\boldsymbol{S} = S_0 \sum_{j=1}^{m} \left[J(j-1) + J(j) \right], \qquad (18)$$

where S_0 is the area of elementary strip on the surface of corona wire $S_0 = \pi r_0 l / m$, l = 1 m, and $J = \rho k E$. Negative ion mobility $k = 2{,}2 \cdot 10^{-4}$ m^2 / Vs is assumed as constant and independent upon ion age. Computed value of linear current density received from Table 3 by using eq. (18) is 1802,1 μA/m. The value of I_0 computed by using analytical formulas in [6] is 1757,1 μA/m. The difference between these values is 2,5 %, but it is only qualitative comparison because the accuracy of computations based upon Deutsch‘s -Popkov‘s assumption is unknown. Experimental value of the linear current density is 1840 μA/m. The difference between this value and the computed one is 4,5 %. The greater value of experimental current is influenced by local sharpnesses of the corona wire surface.

The values of components of the space force on the line $j = 2$ are given in table 4. They are found by multiplying (5) and (6) by the charge density. Line $j = 2$ is chosen because of the component E_φ and subsequently F_φ is equal to 0 on the line $j = 1$. It is necessary to note that the component F_r is dominant for all radial lines of the grid. The difference between the digital values of the component F_r and the corresponding values computed with the Deutsch's-Popkov's assumption in [6] increases from 9,3 % at the corona wire surface to 29,6 % on the surface of plate.

Table 3. Charge density and current density on the surface of corona wire

j	φ, °	ρ, μC/m^3	J, A/m^2
1	0	2951,4	10,26
2	12	2906,2	10,10
3	24	2825,6	9,82
4	36	2639,9	9,18
5	48	2419,9	8,41
6	60	2241,0	7,79
7	72	1995,4	6,94
8	84	1731,2	6,02
9	96	1479,2	5,14
10	108	1259,3	4,38
11	120	1029,0	3,58
12	132	828,6	2,88
13	144	676,4	2,35
14	156	553,1	1,92
15	168	479,1	1,66
16	180	430,7	1,50

The differences between digital and analytical values of the component F_φ are considerably larger. Not only the values of the quantity differ substantially but also the law of its variation along the line of the grid. There are at least two possible reasons of these differences. The first of them may be indicates the weakness of the Deutsch's-Popkov's assumption for the analysis of the corona field in the wire-to-plane electrode system. The second reason may be the imperfection of our computational scheme.

Table 4. Components of the spatial force on the line $j = 2$

r, mm	F_r, N/m^3 accord.[6]	F_r, N/m^3 digital	F_φ, N/m^3 accord.[6]	F_φ, N/m^3 digital
0,050	50915,6	46498,6	-22,1	0
0,060	42116,5	38191,8	-22,1	-0,1
0,073	34841,2	31467,8	-22,1	-0,2
0,088	28825,7	25927,9	-22,2	-0,5
0,107	23852,0	21363,6	-22,2	-1,0
0,129	19739,7	17603,4	-22,2	-1,6
0,156	16339,5	14505,8	-22,3	-2,3
0,189	13528,1	11954,3	-22,4	-3,4
0,229	11203,7	9852,8	-22,4	-4,5
0,279	9281,8	8122,3	-22,5	-6,0
0,335	7692,8	6697,7	-22,6	-7,8
0,405	6379,1	5525,2	-22,7	-10,0
0,490	5293,0	4560,1	-22,9	-12,5
0,592	4395,1	3767,4	-23,1	-15,5
0,716	3652.9	3115,2	-23,4	-18,7
0,866	3039,4	2579,1	-23,6	-22,2
1,048	2532,4	2138,2	-24,0	-25,8
1,267	2113,5	1775,3	-24,5	-29,2
1,533	1767,6	1476,3	-25,0	-32,2
1,854	1482,0	1229,8	-25,7	-34,5
2,242	1246,5	1026,9	-26,6	-36,1
2,712	1052,6	860,2	-27,8	-37,1
3,280	893,2	723,7	-29,3	-37,5
3,966	762,7	612,6	-31,3	-37,8
4,797	656,5	522,5	-33,9	-38,2
5,802	571,0	449,9	-37,6	-39,1
7,017	503,4	392,1	-42,9	-40,7
8,486	451,9	346,8	-50,8	-43,7
10,26	415,8	312,5	-63,6	-48,8
12,00	395,5	278,3	-86,1	-41,9

Conclusions

1. Digital procedure for description of boundary conditions and for computation of direct current two-dimensional corona field by use the finite difference method in polar coordinate system is discussed. Procedure involves the iterative solution of the system of corona field equations comprising the Poisson's equation and the continuity one.
2. The test problem of electrostatic field of two wire transmission line is constructed for checking the reliability of the procedure. Maximum difference between the digital and test problem data for potential at the surface of the wire is only 0,13 %, and it is 6,4 % for field strength (for the number of nodes in computational area equal to 518). It is acceptable for engineering computations.
3. Comparison of digital corona field strength data and the data received by analytical formulas based upon the Deutsch's-Popkov's assumption show that the difference between them varies from 0,3 % at the surface of corona wire to 10,7 % on the surface of the plane electrode. Corresponding results for charge density are 8,1 % and 16,7 %. Results of computation confirm the conclusion of many researchers that the space charge reduces the field strength at the surface of corona wire and increases it at the surface of plane electrode.
4. Digital data of volt-ampere characteristic for the discharge gap differ from analytical ones by 2,5 % and from experimental result by 4,5 % (for the relative corona discharge voltage $U/U_0 = 2{,}05$).
5. The spatial force component F_r is dominant for all radial lines of the grid. The difference between the digital values of the component F_r and the corresponding values computed with the Deutsch's-Popkov's assumption increases from 9,3 % at the corona wire surface to 29,6 % on the surface of plate.

References

1. **Jones J. E.** On Corona–Induced Gas Motion and Heating I: Field Equations, Modelling and Vortex Formation // Journal of Electrostatics. – 2008. – Vol. 66, Iss. 1–2. – P. 84–93.
2. **Atten P., Coulomb J. L., Khaddour B.** Modeling of Electrical Field Modified by Injected Space Charge// IEEE Transactions on Magnetics. – 2005. – Vol. 41, No. 5. – P. 1436–1439.

3. **Al–Hamouz Z. M.** Combined Algorithm Based on Finite Elements and a Modified Method of Characteristics for the Analysis of the Corona in Wire–Duct Electrostatic Precipitators // IEEE Transactions on Industry Applications. – 2002. – Vol. 38, No 1. – P. 43–49.
4. **Marčiulionis P., Žebrauskas S**. Equations of DC Corona Electric Wind Velocities // Electronics and Electrical Engineering. – Kaunas: Technologija, 2007. – No. 8(80). – P. 73–76.
5. **Marčiulionis P., Žebrauskas S**. Electric Force of Unipolar Corona Discharge Causing the Ion–Induced Wind. Proceedings of XVII International Conference on Electromagnetic Disturbances EMD‘2007, September 19–21, 2007, Bialystok, Poland. –P. 1.4–1–1.4–6.
6. **Marčiulionis P., Žebrauskas S**. Computation of Corona Ion–Driven Wind. Proceedings of XVIII International Conference on Electromagnetic Disturbances EMD‘2008, September 25–26, 2008, Vilnius, Lithuania. – P. 213–216.

Received 2009 04 14

P. Marčiulionis, S. Žebrauskas. Numerical Analysis of Spatial Force Components in Direct Current Corona Field // Electronics and Electrical Engineering. – Kaunas: Technologija, 2009. – No. 8(96). – P. 3–8.

Digital procedure for description of boundary conditions and for computation of direct current two-dimensional corona field by use the finite difference method in polar coordinate system is discussed. Procedure involves the iterative solution of the system of corona field equations comprising the Poisson's equation and the continuity one. Maximum difference between the digital and test problem data for electrostatic field potential at the surface of the wire is only 0,13 %, and it is 6,4 % for field strength (for the number of nodes in computational area equal to 518). Comparison of digital corona field strength data and the data received by analytical formulas based upon the Deutsch‘s-Popkov‘s assumption show that the difference between them varies from 0,3 % at the surface of corona wire to 10,7 % on the surface of the plane electrode. Corresponding results for charge density are 8,1 % and 16,7 %. Digital data of volt-ampere characteristic for the discharge gap differ from analytical ones by 2,5 % and from experimental result by 4,5 %. The spatial force component F_r is dominant for all radial lines of the grid. The difference between the digital values of the component F_r and the corresponding values computed by analytical formulas increases from 9,3 % at the corona wire surface to 29,6 % on the surface of plate. Ill. 3, bibl. 6, tabl. 4 (in English; abstracts in English, Russian and Lithuanian).

П. Марчюлёнис, С. Жебраускас. Численный анализ составляющих объёмной силы в поле униполярного коронного разряда // Электроника и электротехника. – Каунас: Технология, 2009. – № 8(96). – С. 3–8.

Обсуждается численная процедура формирования краевых условий и вычисления двухдименсионного униполярного коронного разряда с использованием метода конечных разностей в полярной системе координат. Процедура основана на итерационном решении системы уравнений электрического поля коронного разрядя, состоящей из уравнения Пуассона и уравнения непрерывности. Максимальное различие между численными результатами электростатического поля и данными тестовой задачи составляет 0,13 % по потенциалу и 6,4 % по напряженности поля у поверхности коронирующего провода (при количестве узлов сетки, равном 518). Сравнение численных результатов напряженности электрического поля короны и данных аналитического расчета, основанного на допущении Дейча-Попкова, показывает, что разница между ними возрастает от 0,3 % у поверхности провода до 10,7 % на поверхности плоского электрода. Соответствующие результаты по плотности заряда - 8,1 % и 16,7 %. Численные данные вольтамперной характеристики отличаются от аналитических на 2,5 % и от экспериментальных на 4,5 %. Составляющая F_r обьемной силы доминирует для всех радиальных линий сетки. Разница между численными и аналитическими данными составляющей F_r возрастает от 9,3 % у поверхности провода до 29,6 % на поверхности плоскости. Ил. 3, библ. 6, табл. 4 (на английском языке; рефераты на английском, русском и литовском яз.).

P. Marčiulionis, S. Žebrauskas. Vienpolio vainikinio išlydžio lauko tūrinės jėgos dedamųjų skaitinė analizė // Elektronika ir elektrotechnika. – Kaunas: Technologija, 2009. – Nr. 8(96). – P. 3–8.

Aptariama dvimačio vienpolio vainikinio išlydžio kraštinių sąlygų nustatymo ir išlydžio elektrinio lauko skaičiavimo, taikant baigtinių skirtumų metodą polinėje koordinačių sistemoje procedūra. Ji apima vainikinio išlydžio elektrinio lauko lygčių sistemos, kurią sudaro Poissono ir tolydumo lygtys, iteracinį sprendimą. Didžiausias elektrostatinio lauko potencialo šalia vielinio elektrodo paviršiaus skaitinio rezultato ir testinio uždavinio sprendinio skirtumas yra 0,13 %, lauko stiprio šis skirtumas sudaro 6,4 % (kai tinklelio mazgų skaičius yra 518). Vainikinio išlydžio elektrinio lauko stiprio skaitinio rezultato ir analitinio sprendinio, pagrįsto Deutscho ir Popkovo prielaida, tarpusavio skirtumas didėja nuo 0,3 % prie laido paviršiaus iki 10,7 % plokščiojo elektrodo paviršiuje. Atitinkami krūvio tankio rezultatai yra 8,1 % ir 16,7 %. Voltamperinės charakteristikos skaitinės analizės rezultatai nuo analitinių skiriasi 2,5 %, o nuo eksperimentinių – 4,5 %. Tūrinės jėgos dedamoji F_r vyrauja visose spindulinėse tinklelio linijose. Skaitinių ir analitinių šios jėgos dedamosios verčių skirtumas didėja nuo 9,3 % laido paviršiuje iki 29,6 % plokščiojo elektrodo paviršiuje. Il. 3, bibl. 6, lent. 4 (anglų kalba; santraukos anglų, rusų ir lietuvių k.).